


Communication

# A Smartphone Integrated Platform for Ratiometric Fluorescent Sensitive and Selective Determination of Dipicolinic Acid

Xiang Li <sup>1,\*</sup>, Junsong Wu <sup>2</sup>, Huaguang Hu <sup>1</sup>, Fangfang Liu <sup>1</sup>  and Jialian Wang <sup>1,\*</sup><sup>1</sup> School of Marine and Biological Engineering, Yancheng Teachers University (YCTU), Yancheng 224002, China<sup>2</sup> Department of Basic Medical Science, Jiangsu Vocational College of Medicine, Yancheng 224005, China

\* Correspondence: lix01@yctu.edu.cn (X.L.); wangjl@yctu.edu.cn (J.W.)

**Abstract:** A desirable lanthanide-based ratiometric fluorescence probe was designed as a multifunctional nanoplatform for the determination of dipicolinic acid (DPA), a unique bacterial endospore biomarker, with high selectivity and sensitivity. The carbon dots (CDs) with blue emission wavelengths at 470 nm are developed with europium ion ( $\text{Eu}^{3+}$ ) to form  $\text{Eu}^{3+}/\text{CDs}$  fluorescent probes. DPA can specifically combine with  $\text{Eu}^{3+}$  and then transfer energy from DPA to  $\text{Eu}^{3+}$  sequentially through the antenna effect, resulting in a distinct increase in the red fluorescence emission peak at 615 nm. The fluorescence intensity ratio of  $\text{Eu}^{3+}/\text{CDs}$  (fluorescence intensity at 615 nm/fluorescence intensity at 470 nm) showed good linearity and low detection limit. The developed ratiometric nanoplatform possesses great potential for application in complex matrices owing to its specificity for DPA. In addition, the integration of a smartphone with the Color Picker APP installed enabled point-of-care testing (POCT) with quantitative measurement capabilities, confirming the great potential of the as-prepared measurement platform for on-site testing.

**Keywords:** ratiometric; fluorescence; determination of dipicolinic acid; smartphone-based detection



**Citation:** Li, X.; Wu, J.; Hu, H.; Liu, F.; Wang, J. A Smartphone Integrated Platform for Ratiometric Fluorescent Sensitive and Selective Determination of Dipicolinic Acid. *Biosensors* **2022**, *12*, 668. <https://doi.org/10.3390/bios12080668>

Received: 5 July 2022

Accepted: 17 August 2022

Published: 22 August 2022

**Publisher's Note:** MDPI stays neutral with regard to jurisdictional claims in published maps and institutional affiliations.



**Copyright:** © 2022 by the authors. Licensee MDPI, Basel, Switzerland. This article is an open access article distributed under the terms and conditions of the Creative Commons Attribution (CC BY) license (<https://creativecommons.org/licenses/by/4.0/>).

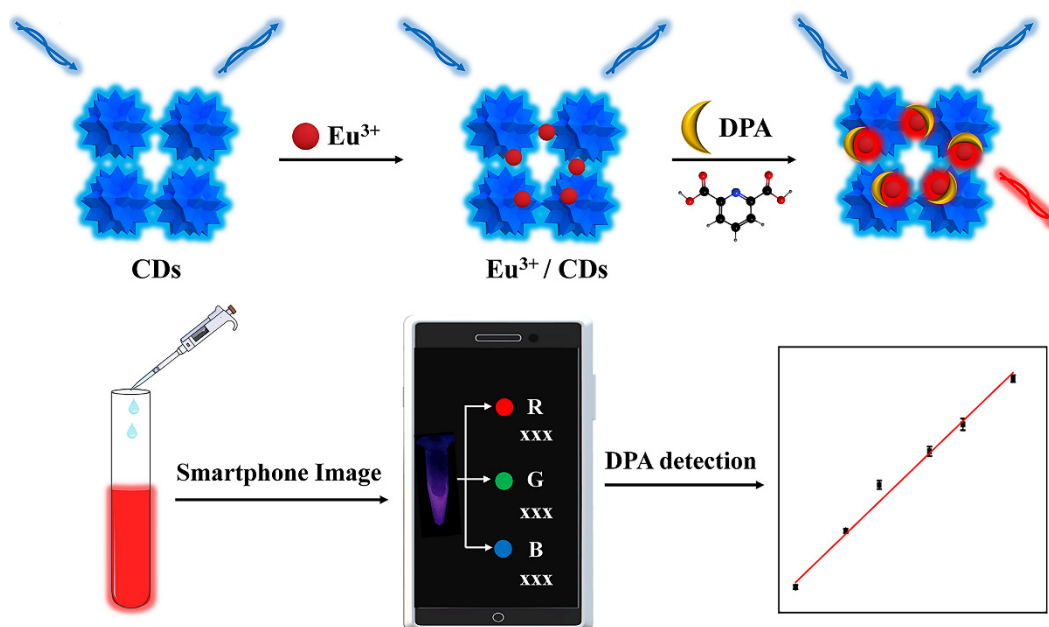
## 1. Introduction

Inhalation of  $10^4$  or more concentration of *Bacillus anthracis* (*B. anthracis*) spores can lead to a mortality of as high as 75%, even within 24 to 48 h of drug treatment [1,2], indicating that *B. anthracis* spores poses a serious threat to human health and public safety [3,4]. Therefore, sensitive and selective determination of *B. anthracis* spores had a critical role to play in early clinical diagnosis and preventing disease outbreaks [5,6]. Dipicolinic acid (DPA), making up approximately 5–15% of the dry weight of anthrax spores, was an extremely important component and major biomarker of anthrax spores [7–10]. Consequently, the level of anthrax spores could be detected and evaluated through the concentration of DPA. Recently, although considerable strategies for the determination of DPA had been constructed, including electrochemical assays, Surface-enhanced Raman spectroscopy (SERS), mass spectrometry (MS), colorimetric methods, etc. [11,12]. These strategies are usually cumbersome, time-consuming and require large instruments, which may not be suitable for on-site rapid detection of DPA. In general, fluorescence-based sensing was a promising optical candidate for addressing the above-mentioned problems in DPA determination [13–15]. However, the further application of fluorescent probes was greatly restricted by the shortcomings of their used currently, such as complicated synthesis processes, poor fluorescence stability and low sensitivity [16].

Lanthanide-based fluorescence nanoprobess had been constructed and employed to the determination of targeting on account of that special optical properties such as large Stokes shifts, long fluorescent lifetimes and high fluorescence stability [17–20]. In fluorescence measurements, DPA acted as a single ligand coordinated with  $\text{Eu}^{3+}$  or terbium ions ( $\text{Tb}^{3+}$ ) and then sensitized lanthanide ions emission by transferring excitation energy to the lanthanide ions by an “antenna effect”, a strategy that can be employed to sensing of

DPA levels [21,22]. Ratiometric fluorescence detection strategies, recording fluorescence emission at two different wavelengths, had attracted increasing attention and interest from researchers because of the increased accuracy and reproducibility of target assays as well as the reduction of false positive or false negative signal results compared to strategies with a single emission signal [23–27].

Herein, a desirable ratiometric fluorescence platform was fabricated for the highly sensitive and selective detection of the *B. anthracis* biomarker DPA by integrating  $\text{Eu}^{3+}$  and CDs ( $\text{Eu}^{3+}/\text{CDs}$ ) in Scheme 1. Taking into consideration fully the coordination binding of DPA to  $\text{Eu}^{3+}$  in the complex of  $\text{Eu}^{3+}/\text{CDs}$ , the formed complex of  $\text{Eu}^{3+}/\text{DPA}$  then emitted a red fluorescence while the blue fluorescence of CDs was not changed. Therefore, the fluorescence ratio ( $F_{615}/F_{470}$ ) of red fluorescence to blue fluorescence as a signal can be augmented with increasing concentrations of DPA. Furthermore, the developed strategy was further utilized for the sensitivity detection of DPA in real samples by integrating a smartphone with Color Picker APP. The ratiometric fluorescence sensing platform based on  $\text{Eu}^{3+}/\text{CDs}$  fluorescent probes has the ability to rapidly detect DPA in the field and thus assess the infection level of anthrax spores, which has great potential in food safety and healthcare.



**Scheme 1.** Illustration of the ratiometric fluorescence sensing for DPA detection.

## 2. Materials and Methods

### 2.1. Materials and Reagents

Chemicals including  $\text{Eu}(\text{NO}_3)_3 \cdot 6\text{H}_2\text{O}$ , dipicolinic acid (DPA) were purchased from Aladdin Reagent Co., Ltd. (Shanghai, China). Polyethylenimine was purchased from Sigma-Aldrich. Citric acid, glutamic acid (Glu), cysteine (Cys), glutathione (GSH), adenosine triphosphate (ATP), sodium chloride (KCl), ferric chloride hexahydrate ( $\text{FeCl}_3 \cdot 6\text{H}_2\text{O}$ ), zinc nitrate ( $\text{ZnNO}_3$ ) and nickel chloride hexahydrate ( $\text{NiCl}_2 \cdot 6\text{H}_2\text{O}$ ) were purchased from Sinopharm Group Chemical Reagent Co., Ltd. Milk was purchased from the local supermarket.

### 2.2. Preparation of CDs

CDs were synthesized according to reported work [28]. First, the citric acid and polyethylenimine was dissolved in 10 mL DI water under stirring. Then, the mixture solution was poured into a poly(p-phenol)-lined stainless-steel autoclave and heated at  $200\text{ }^\circ\text{C}$  for 5 h. After that, the obtained solution was dialyzed to remove unreacted impurities.

### 2.3. Determination of DPA with $\text{Eu}^{3+}$ /CDs Sensing System

To determine the optimal incubation time, the DPA (100  $\mu\text{M}$ ) was incubated and stirred with  $\text{Eu}^{3+}$ /CDs in Phosphate Buffer (PB) (10 mM, pH = 7.5) for different minutes (1–20 min) at 25 °C. Then, the fluorescence intensity of the sensing system was recorded by fluorescence spectrometry at 285 nm excitation. Similarly, only the incubation temperature (25–55 °C) was changed in above sensing system to determine the optimal incubation temperature. After adding  $\text{Eu}^{3+}$ /CDs into PB, the DPA with different concentrations (0–200  $\mu\text{M}$ ) was added above the solution and stirred for 10 min at 25 °C. Then, the fluorescence intensity of the sensing system was recorded by fluorescence spectrometry at 285 nm excitation. For interference experiments, the DPA, GSH, Cys, Glu, ATP,  $\text{Cl}^-$ ,  $\text{Zn}^{2+}$ ,  $\text{Ni}^{2+}$  and  $\text{Fe}^{3+}$  were added to  $\text{Eu}^{3+}$ /CDs solution, respectively. The final concentration of DPA and other interfering substances was 50  $\mu\text{M}$ . Finally, the emission spectra at 285 nm excitation of these reaction solutions were recorded.

### 2.4. DPA Sensing in Real Samples

As for DPA detection in real samples, milk was selected as samples. The purchased milk was treated in the same way as previously reported [29]. In order to remove proteins, the purchased milk was sonicated for 30 min with trichloroacetic acid and then the mixture was centrifuged for 5 min. The filter paper was used to filter the supernatant to remove the lipids. DPA with various concentrations (0, 10, 20 and 50  $\mu\text{M}$ ) was spiked into the treated milk for further analysis, which then were added into the  $\text{Eu}^{3+}$ /CDs sensing system. The fluorescence responses were measured under the excitation at 285 nm after incubating for 10 min.

### 2.5. The Smartphone-Integrated Assay for DPA Detection

For the smartphone-based assay for DPA detection, the samples were incubated with  $\text{Eu}^{3+}$ /CDs and stirred for 10 min. Then, the fluorescent image was recorded and analyzed using the Color Picker APP on the smartphone to access its RGB intensity for analysis. It is worth noting that the samples were placed in a dark lamphouse to avoid environmental interference.

## 3. Results

### 3.1. The Principle of Ratiometric Fluorescence Strategy for DPA Determination

The ligand-containing DPA coordinated with  $\text{Eu}^{3+}$  and the triplet excited state of the ligand transferred energy to the emitting state of  $\text{Eu}^{3+}$  to enhance the fluorescence intensity (Figure S1 in Supplementary), which then directly detect DPA [30,31]. Considering that a single variation in signal was susceptible to environmental interference, a ratiometric fluorescent sensor was constructed to overcome these problems and improve the sensitivity and selectivity. As shown in Figure 1, the CDs emitted bright blue fluorescence at 470 nm (curve a), and its fluorescence intensity was not compromised when adding  $\text{Eu}^{3+}$  (curve b). The blue fluorescence can be obviously observed under the UV irradiation, seen in the insert photos. In the presence of DPA, the combined with the complex of  $\text{Eu}^{3+}$ /CDs can obviously enhance the fluorescence at 615 nm due to the occurrence of antenna effect, while the blue fluorescence kept stability (curve c). The red fluorescence was easily found, seen in the insert photo. Therefore, the ratiometric strategy was established to sense the target based on the ratio of  $F_{615}/F_{470}$  against increasing concentrations of DPA, which also provided the basis for intelligent detection using the smartphone with Color Picker APP. Here, the  $F_{615}$  and  $F_{470}$  were the fluorescence emission intensity of  $\text{Eu}^{3+}$ /DPA at 615 nm and the CDs fluorescence emission intensity at 470 nm, respectively.

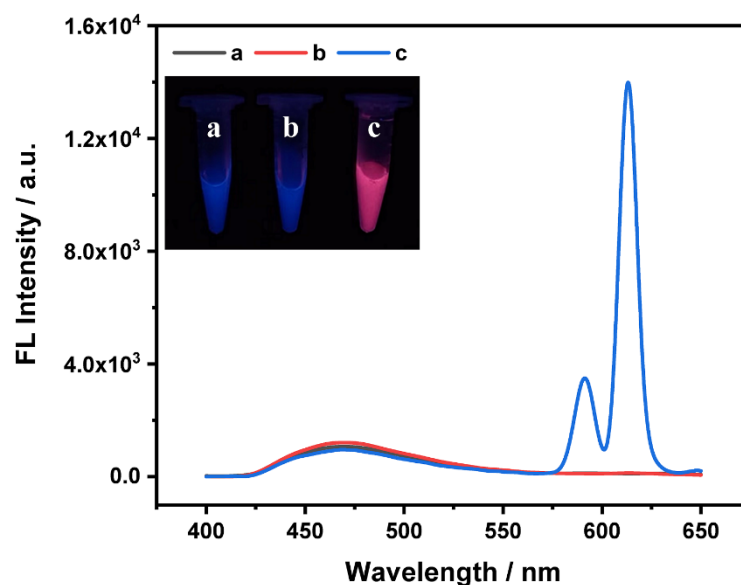


**Figure 1.** The fluorescence spectra and the corresponding photographs of CDs (a), CDs with  $\text{Eu}^{3+}$  (b), and  $\text{Eu}^{3+}$ /CDs with DPA (c).

### 3.2. Optimization of Detection Experimental Conditions

To guarantee the high sensitivity and stability of the  $\text{Eu}^{3+}$ /CDs nanoplatform for target monitoring, several important factors were investigated and optimized, including the concentration of  $\text{Eu}^{3+}$ , reaction temperature and incubation time. The concentration of  $\text{Eu}^{3+}$  was a key factor in the sensitivity of the assays. It can be seen that the blue fluorescent CDs maintains a stable fluorescence intensity with increasing the concentration of  $\text{Eu}^{3+}$  from 0 to 500  $\mu\text{M}$ , which indicates that CDs can be used as an internal parameter (Figure 2A). Due to the energy transfer from DPA to  $\text{Eu}^{3+}$ , the red fluorescence intensity increased significantly after adding different concentrations of  $\text{Eu}^{3+}$  (Figure 2B). The fluorescence ratio of  $F_{615}/F_{470}$  was augmented with concentration of  $\text{Eu}^{3+}$  and reached a plateau at 50  $\mu\text{M}$ . Here, the  $F_{615}$  and  $F_{470}$  were the emitted fluorescence intensity of  $\text{Eu}^{3+}$ /DPA at 615 nm and the CDs at 470 nm, respectively. Thus,  $\text{Eu}^{3+}$  at 50  $\mu\text{M}$  was selected for the detection of DPA in the following experiments. In order to investigate whether the experiment can be performed in the field for rapid detection, the temperature and reaction time of testing were crucial. Learn from Figure 2C,D, the reaction of  $\text{Eu}^{3+}$  and DPA can be carried out rapidly at room temperature and takes only 10 min, indicating that the system had the capability of detecting DPA in a short time and with high stability, providing an important guarantee for subsequent field testing.

### 3.3. The DPA Detection with $\text{Eu}^{3+}$ /CDs Probe

Under the optimal reaction conditions, the detection sensitivity of the as-prepared  $\text{Eu}^{3+}$ /CDs probe was examined by monitoring the ratio fluorescence response of the detection system as a function of different concentrations of DPA in Figure 3A. As the concentration of DPA increased from 0 to 200  $\mu\text{M}$ , the coordination complex  $\text{Eu}^{3+}$ /DPA was formed, resulting in augmented red fluorescence, while the blue emission fluorescence remained relatively constant. To evaluate the sensitivity of the ratiometric fluorescence platform, the ratio of  $F_{615}/F_{470}$  was plotted against different concentrations of DPA, and the variation of ratio in Figure 3B,C was linear over the concentration range of 0–20  $\mu\text{M}$  with a correlation coefficient  $R^2$  of 0.9961 and 20–150  $\mu\text{M}$  with a correlation coefficient  $R^2$  of 0.9971. The limit of detection (LOD) was calculated to be as low as 1.18  $\mu\text{M}$  according to the three times of signal-to-noise ratio, which confirmed the feasibility of the developed platform. The selectivity was further examined by measuring the fluorescence ratio of the system against other potential interfering analytes. As illustrated in Figure 3D, the fluorescence ratio of the target analyte DPA (50  $\mu\text{M}$ ) can be obviously monitored, which

was significantly higher than that of other analytes, which proves that only DPA target can cause the change of sensor signal. Therefore, the developed strategy was specific and selective for the detection of DPA and can greatly reduce the influence of other interferents.

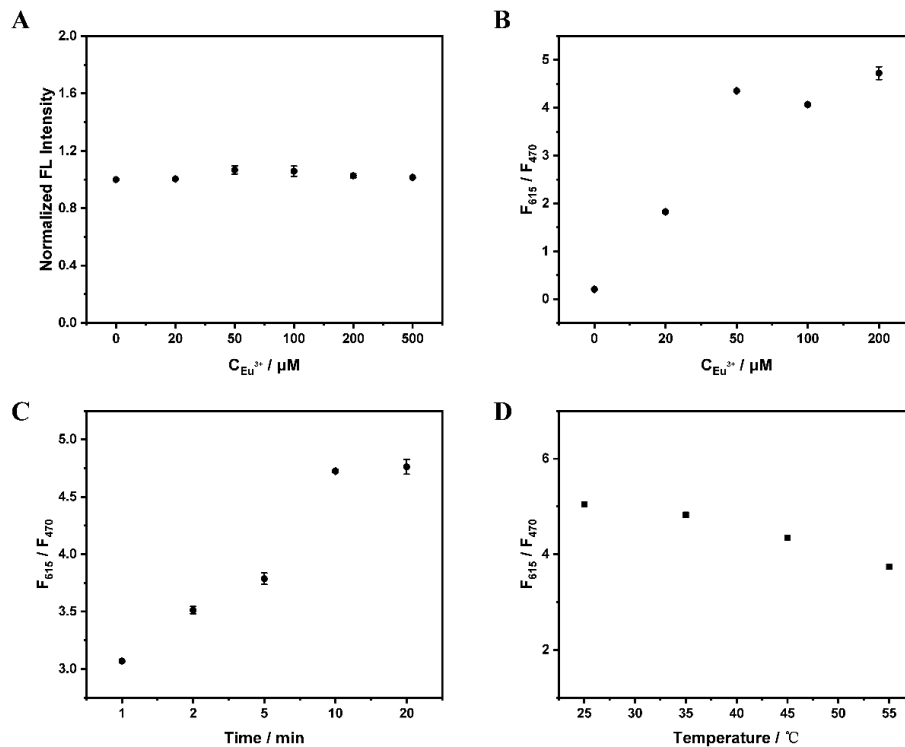


**Figure 2.** (A) The normalized fluorescence intensity of CDs against different concentrations of  $Eu^{3+}$ . (B) The ratio of  $F_{615}/F_{470}$  against different concentrations of  $Eu^{3+}$  in CDs with DPA. The reaction times (C) and different temperature (D) of the  $Eu^{3+}$ /CDs system in the presence of DPA.

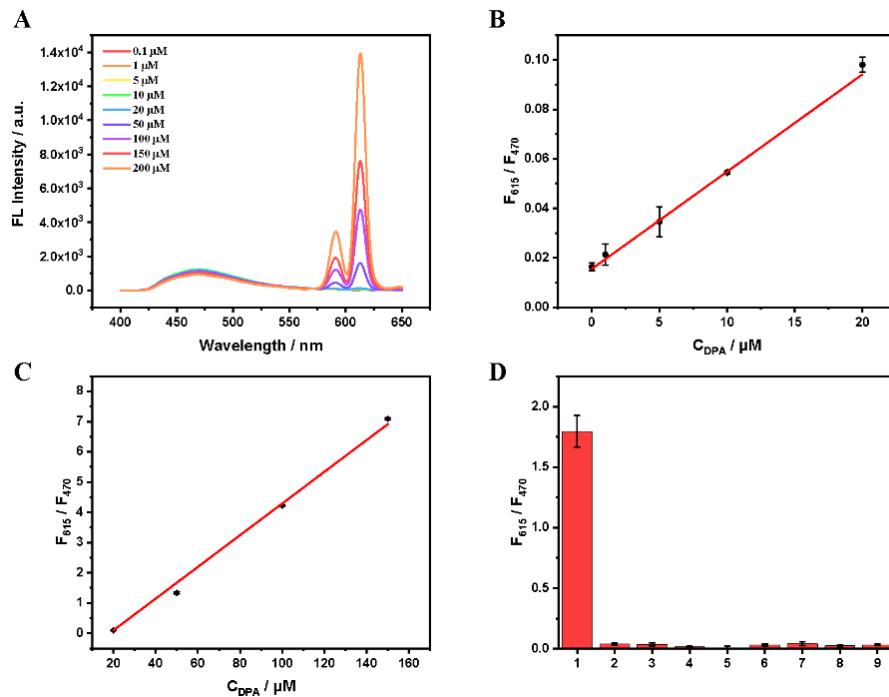


**Figure 3.** (A) The fluorescence spectra of  $Eu^{3+}$ /CDs in the presence of different concentrations of DPA. The standard curves of DPA detection in the range from 0–20  $\mu M$  (B) and 20–150  $\mu M$  (C). (D) Selectivity sensing of the ratiometric fluorescence platform in the presence of each interferential substance and DPA target (1: DPA, 2: Cys, 3: GSH, 4: ATP, 5: Glu, 6:  $Cl^-$ , 7:  $Fe^{3+}$ , 8:  $Zn^{2+}$ , 9:  $Ni^{2+}$ ).

### 3.4. Sensitive Detection of DPA in Real Samples

To further explore the practicality of the proposed strategy, the milk samples with spiking a certain concentration of DPA were selected for the experiment. As displayed in Table 1, no DPA was detected in real samples. Then, the DPA with different concentrations (0, 10, 20, 50  $\mu\text{M}$ ) was spiked into the samples and then the same procedure was followed for quantification by the developed platform. The results showed satisfactory recoveries (97–99%) and accuracy (RSD < 4.05%) for detection of DPA, suggesting that the proposed platform can be used to determination the DPA in real food samples.

**Table 1.** Determination of spiked samples of DPA in real samples by the developed strategy.

Sample	Spiked ( $\mu\text{M}$ )	Found	Recovery (%)	RSD (%)
Milk	0	-	-	-
	10	9.9	99	1.65
	20	19.8	99	4.05
	50	48.5	97	2.9

### 3.5. Smartphone-Integrated DPA Detection in Real Samples

The current fluorescence assays usually require fluorescence spectrometer and specialized researchers, which is not suitable in on-site analysis [32–37]. In this research, a smartphone installed a Color Picker APP is used as a signal reader to detect the DPA by integrating with the as-prepared ratiometric fluorescent sensing, Figure 4A. The color of sample-triggered fluorescence photograph can be converted to digital values representing the blue (B), green (G) and red (R) color channels. The blue fluorescence (Blue channel) can gradually convert red fluorescence (Red channel) with increasing concentration of DPA range from 5 to 150  $\mu\text{M}$  under UV light irradiation. Meanwhile, CIE coordinates can also prove the color changes from blue to red in Figure 4B. As shown in Figure 4A, the ration of red (G) to blue (B) channel (R/B) was linearly related in the range of 5 to 150  $\mu\text{M}$ .

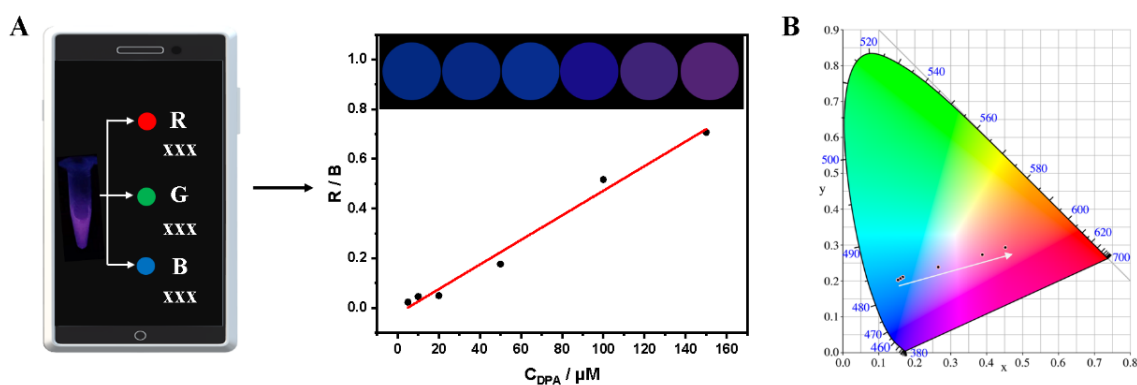


**Figure 4.** The smartphone-based sensor calibration plot based on ratio of R/B (A) and the CIE chromaticity coordinates of  $\text{Eu}^{3+}/\text{CDs}$  (B) against concentrations of DPA range from 5 to 150  $\mu\text{M}$  (Illustration: converted photos of  $\text{Eu}^{3+}/\text{CDs}$  with different concentrations of DPA).

## 4. Conclusions

In summary, a ratiometric fluorescence strategy has been developed for sensitive and selective determination of DPA based on lanthanides-based  $\text{Eu}^{3+}/\text{CDs}$  fluorescent sensor. In addition, the developed strategy can significantly reduce the interface from the complex matrixes and environments and that also improve the practicality and reliability. The determination of DPA is then qualified in real samples, showing the satisfactory recoveries from 97 to 99%. The obtained results of solution fluorescence within increasing concentration of DPA can be quantitatively analyzed by a smartphone loaded Color Picker APP, which can be applied to the POCT with accuracy and stability, exhibiting potential promising application in situ for DPA monitoring.

**Supplementary Materials:** The following supporting information can be downloaded at: <https://www.mdpi.com/article/10.3390/bios12080668/s1>, Figure S1: The fluorescence spectra of (a)  $\text{Eu}^{3+}$ , (b) DPA, and (c)  $\text{Eu}^{3+}$ /DPA.

**Author Contributions:** X.L. Conceptualization, Methodology, Supervision, Funding acquisition, Writing—Review & Editing. J.W. (Junsong Wu) Methodology, Validation. H.H. Methodology, Investigation. F.L. Validation, Investigation, Writing—Original Draft. J.W. (Jialian Wang) Methodology, Supervision, Writing—Review & Editing. All authors have read and agreed to the published version of the manuscript.

**Funding:** This work was supported by the Research on the Open Project program of the Beijing Laboratory of Food Quality and Safety, Beijing Technology and Business University (FQS-202007).

**Institutional Review Board Statement:** Not applicable.

**Data Availability Statement:** Not applicable.

**Conflicts of Interest:** The authors declare no conflict of interest.

## References

1. King, D.; Luna, V.; Cannons, A.; Cattani, J.; Amuso, P. Performance Assessment of Three Commercial Assays for Direct Detection of *Bacillus anthracis* Spores. *J. Clin. Microbiol.* **2003**, *41*, 3454–3455. [[CrossRef](#)] [[PubMed](#)]
2. Hurtle, W.; Bode, E.; Kulesh, D.A.; Kaplan, R.S.; Garrison, J.; Bridge, D.; House, M.; Frye, M.S.; Loveless, B.; Norwood, D. Detection of the *Bacillus anthracis* gyrA Gene by Using a Minor Groove Binder Probe. *J. Clin. Microbiol.* **2004**, *42*, 179–185. [[CrossRef](#)] [[PubMed](#)]
3. Enserink, M. This Time it was Real: Knowledge of Anthrax Put to the Test. *Science* **2001**, *294*, 490–491. [[CrossRef](#)] [[PubMed](#)]
4. Zhang, X.Y.; Zhao, J.; Whitney, A.V.; Elam, J.W.; Duyne, R.P.V. Ultrastable Substrates for Surface-Enhanced Raman Spectroscopy:  $\text{Al}_2\text{O}_3$  Overlayers Fabricated by Atomic Layer Deposition Yield Improved Anthrax Biomarker Detection. *J. Am. Chem. Soc.* **2006**, *128*, 10304–10309. [[CrossRef](#)]
5. Liu, M.L.; Chen, B.B.; He, J.H.; Li, C.M.; Li, Y.F.; Huang, C.Z. Anthrax biomarker: An ultrasensitive fluorescent ratiometry of dipicolinic acid by using terbium (III)-modified carbon dots. *Talanta* **2019**, *191*, 443–448. [[CrossRef](#)]
6. Cheng, H.W.; Huan, S.Y.; Yu, R.Q. Nanoparticle-based substrates for surface-enhanced Raman scattering detection of bacterial spores. *Analyst* **2012**, *137*, 3601–3608. [[CrossRef](#)]
7. Bailey, G.F.; Karp, S.; Sacks, L.E. Ultraviolet-Absorption Spectra of Dry Bacterial Spores. *J. Bacteriol.* **1965**, *89*, 984–987. [[CrossRef](#)]
8. Cable, M.L.; Kirby, J.P.; Sorasaene, K.; Gray, H.B.; Ponce, A. Bacterial Spore Detection by  $[\text{Tb}^{3+}(\text{macrocycle})(\text{dipicolinate})]$  Luminescence. *J. Am. Chem. Soc.* **2007**, *129*, 1474–1475. [[CrossRef](#)]
9. Rode, L.J.; Foster, J.W. Germination of Bacterial Spores by Long-Chain Alkyl Amines. *Nature* **1960**, *188*, 1132–1134. [[CrossRef](#)]
10. Ratiu, I.A.; Bocos-Bintintan, V.; Patrut, A.; Moll, V.H.; Turner, M.; Thomas, C.L.P. Discrimination of bacteria by rapid sensing their metabolic volatiles using an aspiration-type ion mobility spectrometer (a-IMS) and gas chromatography-mass spectrometry GC-MS. *Anal. Chim. Acta* **2017**, *982*, 209–217. [[CrossRef](#)]
11. Li, D.; Truong, T.V.; Bills, T.M.; Holt, B.C.; VanDerwerken, D.N.; Williams, J.R.; Acharya, A.; Robison, R.A.; Tolley, H.D.; Milton, L.; et al. GC/MS Method for Positive Detection of *Bacillus anthracis* Endospores. *Anal. Chem.* **2012**, *84*, 1637–1644. [[CrossRef](#)]
12. Shen, M.L.; Liu, B.; Xu, L.; Jiao, H. Ratiometric fluorescence detection of anthrax biomarker 2,6-dipicolinic acid using hetero MOF sensors through ligand regulation. *J. Mater. Chem. C* **2020**, *8*, 4392–4400. [[CrossRef](#)]
13. Yin, S.N.; Tong, C.L. Europium (III)-Modified Silver Nanoparticles as Ratiometric Colorimetric and Fluorescent Dual-Mode Probes for Selective Detection of Dipicolinic Acid in Bacterial Spores and Lake Waters. *ACS Appl. Nano Mater.* **2021**, *4*, 5469–5477. [[CrossRef](#)]
14. Donmez, M.; Yilmaz, M.D.; Kilbas, B. Fluorescent detection of dipicolinic acid as a biomarker of bacterial spores using lanthanide-chelated gold nanoparticles. *J. Hazard. Mater.* **2017**, *324*, 593–598. [[CrossRef](#)]
15. Xu, J.; Shen, X.K.; Jia, L.; Zhang, M.M.; Zhou, T.; Wei, Y.K. Facile ratiometric fluorapatite nanoprobe for rapid and sensitive bacterial spore biomarker detection. *Biosens. Bioelectron.* **2017**, *87*, 991–997. [[CrossRef](#)]
16. Xiu, L.F.; Huang, K.Y.; Zhu, C.T.; Zhang, Q.; Peng, H.P.; Xia, X.H.; Chen, W.; Deng, H.H. Rare-Earth  $\text{Eu}^{3+}$ /Gold Nanocluster Ensemble-Based Fluorescent Photoinduced Electron Transfer Sensor for Biomarker Dipicolinic Acid Detection. *Langmuir* **2021**, *37*, 949–956. [[CrossRef](#)]
17. Donmez, M.; Oktem, H.A.; Yilmaz, M.D. Ratiometric fluorescence detection of an anthrax biomarker with  $\text{Eu}^{3+}$ -chelated chitosan biopolymers. *Carbohydr. Polym.* **2018**, *180*, 226–230. [[CrossRef](#)]
18. Yang, Z.R.; Wang, M.M.; Wang, X.S.; Yin, X.B. Boric-Acid-Functional Lanthanide Metal-Organic Frameworks for Selective Ratiometric Fluorescence Detection of Fluoride Ions. *Anal. Chem.* **2017**, *89*, 1930–1936. [[CrossRef](#)]
19. Rong, M.C.; Deng, X.Z.; Chi, S.T.; Huang, L.Z.; Zhou, Y.B.; Shen, Y.N.; Chen, X. Ratiometric fluorometric determination of the anthrax biomarker 2, 6-dipicolinic acid by using europium (III)-doped carbon dots in a test stripe. *Microchim. Acta* **2018**, *185*, 201. [[CrossRef](#)]

20. Yilmaz, M.D.; Oktem, H.A. Eriochrome Black T-Eu<sup>3+</sup> Complex as a Ratiometric Colorimetric and Fluorescent Probe for the Detection of Dipicolinic Acid, a Biomarker of Bacterial Spores. *Anal. Chem.* **2018**, *90*, 4221–4225. [[CrossRef](#)]
21. Zhang, X.Y.; Young, M.A.; Lyandres, O.; Duyne, R.P.V. Rapid Detection of an Anthrax Biomarker by Surface-Enhanced Raman Spectroscopy. *J. Am. Chem. Soc.* **2005**, *127*, 4484–4489. [[CrossRef](#)]
22. Ai, K.; Zhang, B.H.; Lu, L.H. Europium-based fluorescence nanoparticle sensor for rapid and ultrasensitive detection of an anthrax biomarker. *Angew. Chem. Int. Ed.* **2009**, *48*, 304–308. [[CrossRef](#)]
23. Lee, M.H.; Kim, J.S.; Sessler, J.L. Small molecule-based ratiometric fluorescence probes for cations, anions, and biomolecules. *Chem. Soc. Rev.* **2015**, *44*, 4185–4191. [[CrossRef](#)]
24. Li, Y.Y.; Du, Q.Q.; Zhang, X.D.; Huang, Y.M. Ratiometric detection of tetracycline based on gold nanocluster enhanced Eu<sup>3+</sup> fluorescence. *Talanta* **2020**, *206*, 120202. [[CrossRef](#)]
25. Yan, X.; Li, H.X.; Zheng, W.S.; Su, X.G. Visual and Fluorescent Detection of Tyrosinase Activity by Using a Dual-Emission Ratiometric Fluorescence Probe. *Anal. Chem.* **2015**, *87*, 904–8909. [[CrossRef](#)]
26. Wen, J.L.; Li, N.; Li, D.; Zhang, M.M.; Lin, Y.W.; Liu, Z.; Lin, X.; Shui, L. Cesium-Doped Graphene Quantum Dots as Ratiometric Fluorescence Sensors for Blood Glucose Detection. *ACS Appl. Nano Mater.* **2021**, *4*, 8437–8446. [[CrossRef](#)]
27. Zhan, Y.J.; Yang, S.T.; Chen, L.F.; Zeng, Y.B.; Li, L.; Lin, Z.Y.; Guo, L.H.; Xu, W. Ultrahigh Efficient FRET Ratiometric Fluorescence Biosensor for Visual Detection of Alkaline Phosphatase Activity and Its Inhibitor. *ACS Sustain. Chem. Eng.* **2021**, *9*, 12922–12929. [[CrossRef](#)]
28. Hao, T.; Wei, X.; Nie, Y.; Xu, Y.; Yan, Y.; Zhou, J. An eco-friendly molecularly imprinted fluorescence composite material based on carbon dots for fluorescent detection of 4-nitrophenol. *Microchim. Acta* **2016**, *183*, 2197–2203. [[CrossRef](#)]
29. Wang, T.L.; Mei, Q.S.; Tao, Z.H.; Wu, H.T.; Zhao, M.Y.; Wang, S.; Liu, Y.Q. A smartphone-integrated ratiometric fluorescence sensing platform for visual and quantitative point-of-care testing of tetracycline. *Biosens. Bioelectron.* **2020**, *148*, 111791. [[CrossRef](#)]
30. Li, X.Q.; Luo, J.J.; Deng, L.; Ma, F.H.; Yang, M.H. In situ incorporation of fluorophores in zeolitic imidazolate framework-8 (ZIF-8) for ratio-dependent detecting a biomarker of anthrax spores. *Anal. Chem.* **2020**, *92*, 7114–7122. [[CrossRef](#)]
31. Zhao, J.H.; Wang, S.; Lu, S.S.; Sun, J.; Yang, X.R. A luminescent europium-dipicolinic acid nanohybrid for the rapid and selective sensing of pyrophosphate and alkaline phosphatase activity. *Nanoscale* **2018**, *10*, 7163–7170. [[CrossRef](#)]
32. Wang, T.L.; Ji, X.Y.; Tao, Z.H.; Zhou, X.; Hao, Z.; Wang, X.K.; Gao, X.; Wang, S.; Liu, Y.Q. Dual stimuli-responsive lanthanide-based phosphors for an advanced full-color anti-counterfeiting system. *RSC Adv.* **2020**, *10*, 15573–15578. [[CrossRef](#)]
33. Liu, X.W.; Li, X.; Xu, S.L.; Guo, S.J.; Xue, Q.W.; Wang, H.S. Efficient ratiometric fluorescence probe based on dual-emission luminescent lanthanide coordination polymer for amyloid  $\beta$ -peptide detection. *Sens. Actuators B Chem.* **2021**, *352*, 131052. [[CrossRef](#)]
34. Hussain, S.; Chen, X.; Wang, C.F.; Hao, Y.; Tian, X.M.; He, Y.L.; Li, J.; Shahid, M.; Iyer, P.K.; Gao, R.X. Aggregation and Binding-Directed FRET Modulation of Conjugated Polymer Materials for Selective and Point-of-Care Monitoring of Serum Albumins. *Anal. Chem.* **2022**, *94*, 10685–10694. [[CrossRef](#)]
35. Hussain, S.; Malika, A.H.; Iyer, P.K. FRET-assisted selective detection of flavins via cationic conjugated polyelectrolyte under physiological conditions. *J. Mater. Chem. B* **2016**, *4*, 4439–4446. [[CrossRef](#)]
36. Malik, A.K.; Hussain, S.; Iyer, P.K. Aggregation-Induced FRET via Polymer-Surfactant Complexation: A New Strategy for the Detection of Spermine. *Anal. Chem.* **2016**, *88*, 7358–7364. [[CrossRef](#)]
37. Mondal, S.; Zehra, N.; Choudhury, A.; Iyer, P.K. Wearable Sensing Devices for Point of Care Diagnostics. *ACS Appl. Bio Mater.* **2021**, *4*, 47–70. [[CrossRef](#)]